

# Accurate binding of calcium to phospholipid bilayers by effective inclusion of electronic polarization

Josef Melcr and Hector Martinez-Seara Monne

*Institute of Organic Chemistry and Biochemistry, Academy of Sciences of the Czech Republic, Prague 6, Czech Republic*

Pavel Jungwirth

*Institute of Organic Chemistry and Biochemistry, Academy of Sciences of the Czech Republic, Prague 6, Czech Republic and  
Department of Physics, Tampere University of Technology, P.O. Box 692, FI-33101 Tampere, Finland*

O. H. Samuli Ollila\*

*Institute of Organic Chemistry and Biochemistry, Academy of Sciences of the Czech Republic, Prague 6, Czech Republic and  
Institute of Biotechnology, University of Helsinki*

(Dated: October 18, 2017)

Despite of the significant biological relevance, the binding details of cations in cellular lipid membranes are not fully understood. For example, consistent results for the binding affinities and stoichiometries of  $\text{Na}^+$  and  $\text{Ca}^{2+}$  ions to phospholipid bilayers have not been achieved with different experimental and theoretical methods. As recently shown in the NMRlipids project, a Open Collaboration running at [nmrlipids.blogspot.com](http://nmrlipids.blogspot.com), the ion binding details could be resolved with unprecedented detail by interpreting the experimental NMR data with classical molecular dynamics (MD) simulations. However, the accuracy of the existing lipid models for MD simulations was not sufficient for this. In this work we show that the binding details of  $\text{Na}^+$  and  $\text{Ca}^{2+}$  ions to 1-Palmitoyl-2-oleoylphosphatidylcholine (POPC) bilayer can be accurately described with a MD simulation model having implicitly included electronic polarization. This is demonstrated by applying the electronic continuum correction (ECC) to a state of the art lipid model for MD simulations of POPC lipid bilayer. The introduced ECC-lipid model reproduces the experimentally measured structural parameters for the ion-free membrane, the response of lipid headgroup to the bound positive charge, and the binding affinities of  $\text{Na}^+$  and  $\text{Ca}^{2+}$  ions. The imperceptible binding of  $\text{Na}^+$  ions to POPC bilayer and interactions of  $\text{Ca}^{2+}$  mainly with phosphate oxygens in the ECC-lipid model give support to the early interpretations of the experimental spectroscopic data. On the other hand,  $\text{Ca}^{2+}$  ions form complexes with 1-3 lipid molecules with almost equal probabilities, suggesting more complicated binding stoichiometry than the simple binding model used to interpret the NMR data. The results in this work pave the way for MD simulations of complex biochemical systems with realistic electrostatic interactions in the vicinity of cellular membranes.

## I. INTRODUCTION

Cation interactions with cellular membranes play a key role in several biological processes, such as in signal propagation in neurons and vesicle fusion. Since the direct measurements of ion-membrane interactions from biological systems are difficult, lipid bilayers are often used as models systems for cellular membranes. Especially the zwitterionic phosphocholine (PC) lipid bilayers are used to understand the role of ions in complex biological systems [1–3].

Interactions of biological cations, especially  $\text{Na}^+$  and  $\text{Ca}^{2+}$ , with PC bilayers are widely studied in experiments [2–9] and classical MD simulations [10–14]. The details of ion binding are, however, not fully consistent in the literature. Interpretations of non-invasive spectroscopic methods, like nuclear magnetic resonance (NMR), scattering and infrared spectroscopy suggest that  $\text{Na}^+$  ions exhibit negligible binding to PC lipid bilayers with submolar concentrations, while  $\text{Ca}^{2+}$  specifically binds to phosphate groups of two lipid molecules [4, 5, 7–9, 15–17]. Atomistic resolution molecular dynamics (MD) simulation models, however, predict significantly stronger binding for the cations than NMR experiments [18]. On the other hand, some experiments have also

been interpreted to support the predictions from MD simulations [10, 19]. Furthermore, interactions of Calcium ions with 3-4 lipids, including also interactions with carbonyl oxygens, have been reported from simulations [10, 11, 13, 14].

Recent work published by the NMRlipids project ([nmrlipids.blogspot.fi](http://nmrlipids.blogspot.fi)) [18] made an attempt to resolve the apparent controversies. A direct comparison of ion binding affinities to PC bilayers was presented between simulations and experiments by using the electrometer concept, which is based on the experimental NMR data for the lipid headgroup order parameters [20]. Using massive amounts of data collected by Open Collaboration method, it was concluded that the accuracy of the current state of the art lipid models for MD simulations is not sufficient for the detailed interpretation of the cation interactions with PC lipid bilayers [18].

In this work we show that the cation binding behavior in MD simulations of 1-Palmitoyl-2-oleoylphosphatidylcholine (POPC) bilayer can be significantly improved by implicitly including the electronic polarizability in the polar region of lipid molecules. The electronic polarizability is included by using the electronic continuum correction (ECC) [21], which has been previously shown to improve the behaviour of MD simulations of ions in bulk water [22–24]. As a starting point we use the parameters from the Lipid14 model [25], which gave the best cation binding behaviour in the previous study [18]. The developed ECC-lipid parameters reproduce the ex-

---

\*samuli.ollila@helsinki.fi

perimentally measurable structural parameters of an ion-free POPC lipid bilayer with the accuracy comparable to the other state of the art lipid models, while surpassing them significantly for reproducing the membrane binding affinities and induced structural effects of Sodium and Calcium ions.

## II. METHODS

### A. Electronic continuum correction for lipid bilayers

The lack of electronic polarizability in the standard MD simulation force fields has been considered a highly relevant issue since the early days of lipid bilayer simulations. In this work we circumvent the rather demanding explicit inclusion of electronic polarization effects [26] by implicitly including electronic polarizability in lipid bilayer simulations by using the electronic continuum correction (ECC) [21]. Technically, it is a similar approach to the phenomenological charge-scaling as applied in earlier studies [27, 28]. **1. We should also cite papers where empirical scaling was used ionic liquids DOI: 10.1002/anie.201308760** The present concept of ECC is, however, physically well justified and rigorously derived [21, 29, 30].

Following the ECC concept, electronic polarizability can be effectively included in classical MD simulations by placing all particles into a homogeneous dielectric continuum with a dielectric constant  $\epsilon_{el}$ , which is the electronic part of the dielectric constant of the media [21]. Measurements of high frequency dielectric constant gives values around 2 for almost any biologically relevant material [21? ]. Following the Coulomb's law, such a dielectric continuum can be easily included in standard MD simulation by a scaling of charges

$$Q^{ECC} = f_q \cdot Q \quad (1)$$

with a constant scaling factor  $f_q = \epsilon_{el}^{-1/2}$  effectively representing the newly introduced electronic continuum. Given the high frequency dielectric constant as measured in water (corresponding to the square of the refraction index) of  $\epsilon_{el} = 1.78$ , the scaling factor for aqueous ions is  $f_q = 0.75$  [21? ]. This scaling factor has been successfully used to improve the performance of force field for ions in solution [23? , 24] which then agree quantitatively with neutron scattering data [22–24].

While the scaling factor of  $f_q = 0.75$  for ions in water improves their description and is physically well justified within the ECC theory [? ], it is nota priori clear whether the same factor should be used for partial charges in molecules, e.g., lipids in our case. Unlike the total charge of an atom or molecules, atomic partial charges within molecules are not physical observables. There are thus several schemes for the assignment of partial charges for biomolecules. [31] Currently, the most commonly employed scheme is the restrained electrostatic potential (RESP) method [32, 33]. By construction, partial charges currently implemented in force fields may already include to some extent the solvent electronic polarizability effects, i.e., the RESP charges are often scaled to fit certain experimental observables **2. This needs a citation - Joe please pick 1-2 papers.** Thus, a consistent application of the ECC scal-

ing factor,  $f_q$ , to the molecular partial charges included in the available force fields does not necessarily have to follow the above relation  $f_q = \epsilon_{el}^{-1/2}$ , but instead it lies between 0.75 i.e., (no electronic polarizability included in the original partial charges) and 1 (i.e., electronic polarizability fully included in the original partial charges).

In this work, we develop a phospholipid model for classical MD simulations that accurately describes the lipid head group response to varying concentrations of monovalent and divalent cations. This is a biologically highly relevant membrane feature, which is poorly reproduced by currently available models. This can affect not only on membrane properties in the presence of ions but also modulate interactions with charged moieties at the interface.

Importantly, results from simulations can be directly compared against experimental NMR data [4, 5, 34], as discussed in detail in Ref. 18. To this end, we explore the above discussed scaling factor parameter space,  $f_q \in (0.75, 1.0)$  for the Lipid14 [25] force field. We selected this force field as a starting point because its response to bound ions was apparently the most realistic against NMR data in a recent test within NMRlipids project (see Fig. 5 in Ref. 18). Moreover, the glycerol backbone and head group structures in Lipid14 model were more realistically described compared with other state of the art lipid models [35]. The ECC correction was applied to Lipid14 parameters by scaling partial charges of the head group, glycerol backbone, and carbonyl regions, which are the most polar parts in the lipids and are thus expected to have the largest contribution to the cation binding. In contrast, we do not modify the hydrocarbon chain parameters, as they do not come in direct contact with salt ions and are already highly optimized to provide a good description for the hydrophobic part of lipid bilayers [36]. This is in contrasts with the behavior in glycerol backbone and head group order parameters in the presence of ions, which call for improvements in all available lipid models [35].

Exploring different values of the scaling factor, we found out that ion bindings and the related head group order parameter responses become weakened in general. The optimal behaviour was observed for a scaling factor of  $f_q = 0.8$ . This value is only slightly higher than the original scaling factor of 0.75, which implies that electronic polarization effects are only to a small extent effectively accounted for in the Lipid14 force field.

While, the above charge scaling improved the description of lipid-ion interactions, it also led to a reduction of the area per molecule of the lipid bilayer in water below experimental values. Simulations with Lipid14 parameters having partial charges of head group, glycerol backbone and carbonyls scaled with 0.8 gave the area per molecule value of  $\approx 60 \text{ \AA}^2$ , as well as which is somewhat smaller than the experimental value of  $64.3 \text{ \AA}^2$  ([3.missing REF for APL experiment]) the Lipid14 value of  $(65.6 \pm 0.5) \text{ \AA}^2$  [25]. The decrease of the area per lipid is found to arise from a reduced hydration of the lipid head group region, due to the lower polarity of molecules with scaled charges. This can be compensated by reducing the effective radius of atoms with scaled charges by changing the  $\sigma$  parameters in the Lennard-Jones potential, as done pre-

viously for ions in solution [22–24]. 4. We should discuss how this can potentially affect the intermolecular interaction when mixing scaled and non scaled molecules.

JOE: I think that we rather increasingly see that there's nothing like "fully non-scaled" with the exception of ions with integer charges. So the discussion shall be rather more about the interaction of our "scaled" (I'd still rather call it ECC-corrected or whatever) and "semi-scaled" models.

SAMULI: There is now a paragraph in the conclusions, which mentions this topic. After reducing these  $\sigma$  parameters by a factor of  $f_\sigma = 0.89$ , the area per molecule is restored back close to the experimental value (see Table I).

## B. Electrometer concept

Ion binding in lipid bilayers was compared between experiments and simulations by using the lipid head group order parameters and the "electrometer concept" [18, 20], which is based on the experimental observation that the C-H bond order parameters of  $\alpha$  and  $\beta$  carbons in PC lipid head group (see Fig. 1) are proportional to the amount of unit charge bound per lipid [20]. The change of order parameters measured with varying aqueous ion concentration can be then related to the amount of bound ions.

The concept can be used to compare the ion binding affinity to lipid bilayers between MD simulations and NMR experiments, because the order parameters can be accurately determined from both techniques [18, 36]. The order parameters for all C-H bonds in lipid molecules, including  $\alpha$  and  $\beta$  segments in head group, can be accurately measured using  $^2\text{H}$  NMR or  $^{13}\text{C}$  NMR techniques [36]. From MD simulations the order parameters can be calculated using the definition

$$S_{\text{CH}} = \frac{3}{2} \langle \cos^2 \theta - 1 \rangle, \quad (2)$$

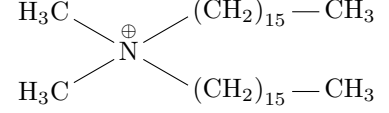
where  $\theta$  is the angle between the bond and membrane normal and the average is taken over all sampled configurations [36].

The relation between bound charge per lipid,  $X^\pm$ , and the head group order parameter change,  $\Delta S_{\text{CH}}^i$ , is empirically quantified as [20, 40]

$$\Delta S_{\text{CH}}^i = S_{\text{CH}}^i(X^\pm) - S_{\text{CH}}^i(0) \approx \frac{4m_i}{3\chi} X^\pm, \quad (3)$$

where  $S_{\text{CH}}^i(0)$  denote the order parameter in the absence of bound charge,  $i$  refers to either  $\alpha$  or  $\beta$  carbon,  $m_i$  is an empirical constant depending on the valency and position of the bound charge, and the experimental value [41, 42],  $\chi \approx 167 \text{ kHz}$ , is used for the quadrupole coupling constant. Atomic absorption spectra and  $^2\text{H}$  NMR data gave  $m_\alpha = -20.5 \text{ kHz}$  and  $m_\beta = -10.0 \text{ kHz}$  for the binding of  $\text{Ca}^{2+}$  to POPC bilayer (in the presence of 100 mM NaCl) [5, 18, 36]. The slopes are negative, because the head group order parameters decrease with bound positive charge and increase with bound negative charge [18, 36]. This can be rationalized as a change of the lipid head group dipole tilt toward water phase with the bound positive charge and *vice versa* with the negative charge [20].

The measured order parameter change depends on both, the head group response to the bound charge and the amount of bound charge, i.e.  $m_i$  and  $X^\pm$  in Eq. 3, respectively. The former property has to be well quantified before the electrometer concept can be used to analyze the binding affinities, as done experimentally for a wide range of systems [20, 43]. To calibrate the head group order parameter response to the bound charge in simulations, we use the experimental data for dihexadecyldimethylammoniumbromide mixed within a POPC bilayer [34]. Dihexadecyldimethylammonium



is a cation surfactant having two acyl chains and bearing a unit charge in the hydrophilic end. Thus, it is expected to locate in the bilayer similarly to the phospholipids and the molar ratio then gives directly the amount of bound unit charge per lipid  $X^\pm$  in these systems [34].

## C. Salt concentrations and binding affinity

The early experimental electrometer concept data for the lipid head group order parameter changes was reported as a function of the salt concentration in water before solvating the lipids [4]. The later study used atomic absorption spectroscopy and reported the order parameter changes as a function of the salt concentration in the supernatant after the solvation of lipids [5]. In this work we focus on POPC for which the latter definition was used [5]. The salt concentration in the aqueous bulk region was calculated from the farthest point from both lipid leaflets in the water phase. Note that in the previous study, Ref. 18, the ion concentrations were calculated in water before solvating the lipids as in the earlier experiments [4]. Despite of the measurable differences between these two definitions of concentrations for  $\text{CaCl}_2$  systems, the qualitative conclusions in this or in the previous work [18] are not affected by this.

To quantify the ion binding affinity to a lipid bilayer, we calculated the relative surface excess of ions with respect to water,  $\Gamma_i^w$  [44]. This quantity was chosen because it does not depend on the position of the Gibbs dividing plane between two bulk regions. Here we assume that the interface locates between the hydrophobic interior of a lipid bilayer and the bulk water region far from the membrane. The bulk concentration of ions and water is zero inside the bilayer. The concentrations in bulk water region can be calculated from the farthest point from both lipid leaflets in the water phase. The region between these boundaries contains all the ions and water molecules in the simulation box. This setup provides a simplified relation for  $\Gamma_i^w$  in lipid bilayers simulations

$$\Gamma_i^w = \frac{1}{2A_b} \left( n_i - n_w \frac{C_i}{C_w} \right), \quad (4)$$

where  $n_w$  and  $n_i$  are the total number of waters and ions in the system;  $C_w$  and  $C_i$  are their respective bulk concentrations in the aqueous phase; and  $A_b$  is the area of the box in the membrane plane. The total area of the interface is twice the area of the membrane,  $2A_b$ , because bilayers have an interface at both leaflets.

#### D. Validation of lipid bilayer structure against experiments

The structure of lipid bilayers in simulations without ions were validated against NMR and x-ray scattering experiments by calculating the order parameters for C-H bonds and the scattering form factors. The former validates the structures sampled by the individual lipid molecules in simulations with atomic resolution, while the latter validates the dimensions of the lipid bilayer (thickness and area per molecule) [36].

The order parameters were calculated from simulations for all C-H bonds in lipid molecules by using Eq. 2. Form factors were calculated from equation 5. *As Hector suggested, it might be better to write the simpler form for this equation.*

$$F(q) = \int_{-D/2}^{D/2} \left( \sum_{\alpha} f_{\alpha}(q_z) n_{\alpha}(z) - \rho_s \right) \exp(izq_z) dz, \quad (5)$$

where  $f_{\alpha}(q_z)$  is the density of atomic scattering length,  $\rho_s$  is the density of solvent scattering length in the bulk region,  $n_{\alpha}(z)$  is the number density of atom  $\alpha$  and  $z$  is the distance from the membrane centre along its normal spanning until the water bulk region,  $D$ .

#### E. Simulation details

##### 1. Simulations of POPC bilayers in aqueous ions

Simulations of POPC bilayer in pure water or in varying salt concentrations contained 128 POPC molecules and approximately 50 water molecules per each lipid in the periodic orthorhombic simulation box. As a default, water molecules were described by the OPC3 force field [45] which is currently the most accurate three site rigid water model. *6. More justification for the choosing the OPC3 water model are needed. It might be good to show the comparison with the scattering data in bulk water in SI.* In order to test transferability of our newly developed ECC-lipids model, we also performed several additional simulations with OPC [46], SPC/E [47], TIP3p-FB and TIP4p-FB [48], and TIP4p/2005 [49] water models. *7. The normal TIP3P was tested as well, right?* presented in Supporting Information (SI). The ECC-ion models were used for Sodium, Calcium and Chloride ions [22, 24? ]. Simulation with the Lipid14 model was also ran with the ion model by Dang et al. [50–52]. Simulation data for the Lipid14 model with Åqvist [53] ion model was taken directly from [54]. *8. Which water model was used in these simulations?* MD simulations were performed using the GROMACS [55] simulation package (version 5.1.4). The simulation settings used in this work are summarized in Table IV. Simulation trajectories and parameters are available at [?] *9. To be uploaded to Zenodo.*

TABLE I: Area per lipid (APL) values of POPC with no ions from the Lipid14 simulation ran in this work and from the literature, from ECC-lipid model and from experiments.

model	APL (Å <sup>2</sup> )	Temperature [K]
Lipid14	65.1 ± 0.6	300
Lipid14 [25]	65.6 ± 0.5	303
ECC-lipids	62.2 ± 0.6	300
experiment [60] <b>19. REF</b>	64.3	303

##### 2. Simulations of POPC bilayers with cationic surfactants

An automated topology builder [56] was first used to create the structure of dihexadecyldimethylammonium. The Amber-Tools program [57] was then used to generate the Amber-type force field parameters. The parameters were converted to the Gromacs format by using the acpype tool [58]. The partial charges were then manually modified to approximately correspond to their equivalent segments in Lipid14 [25]. The parameters are available at [?] *10. To be added.* The surfactants were randomly placed among the lipids to form bilayer structures with mole fractions of 10%, 20%, 30%, 42%, or 50% of surfactant in the POPC bilayer. All systems contained 50 POPC molecules per leaflet, 6340 TIP3P water molecules and 6, 14, 21, 35, or 50 surfactants per leaflet. Chloride counter ions were used in simulations, because parameters for bromide, the counterion in the experimental data [34], were not available in the standard Gromacs files for Amber force field.

*11. JOE: We cannot present an intricate cool new model for a lipid and claim at the same time that we can't simulate bromide.* The Lipid14 model was used for POPC. The first 20 ns of the total simulation time of 200 ns was considered as an equilibration time and was omitted from the analysis. A reasonable lipid neighbor exchange occurred during the simulation.

The same systems were also simulated with the ECC-lipid model for POPC using the same setup. *12. Which water model was used in these simulations?* In these simulations the ECC correction was also applied to the cationic surfactant by scaling all charges with the same factor as for ECC-lipids, i.e.,  $f_q = 0.8$ , and by using the atom types with reduced  $\sigma$  parameters from ECC-lipids. *13. Parameters are available at ??*

### III. RESULTS AND DISCUSSION

#### A. POPC membrane structure and dynamics

The ECC-lipid and Lipid14 models reproduce the experimental x-ray scattering form factors of POPC bilayer with the similar accuracy in Fig. 1. The area per lipid values from the Lipid14 model is slightly larger than the experimental value in Table I, while the value from ECC-lipid model is slightly smaller. Area per lipid values of the ECC-lipid model show some variation when simulated with different water models in Table III (Supplementary Information), however, all the values are close to the experimentally reported values. In con-



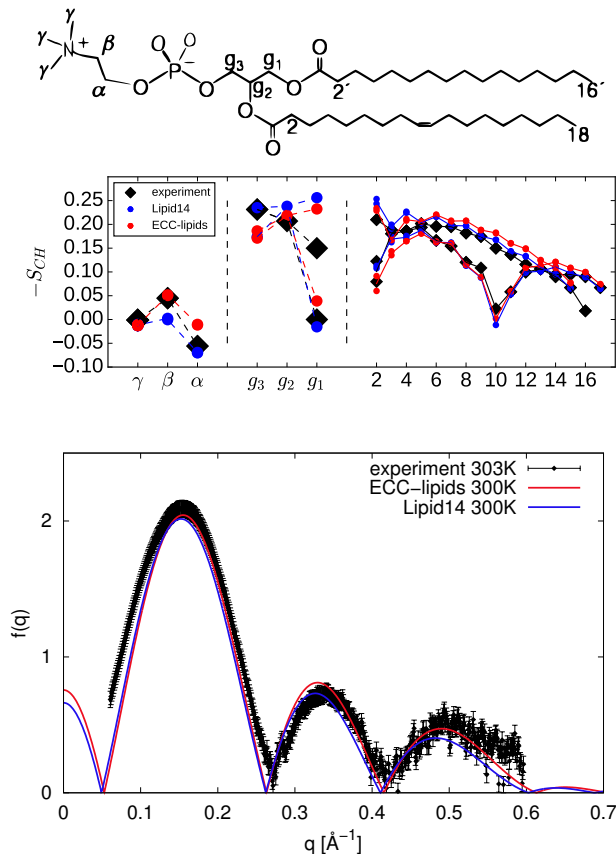


FIG. 1: Top: The chemical structure of POPC and the labeling of the carbon segments. Middle: Order parameters of POPC head group, glycerol backbone and acyl chains from simulations with the Lipid14 [25] and the ECC-lipid models compared with the experimental values from [59]. The size of the points for the head group order parameters correspond to the error bars ( $\pm 0.02$  for experiments [35, 36] and ?? for simulations). The size of the points for acyl chains are decreased by a factor of 3 to improve the clarity of the plot. Bottom: X-ray scattering form factors from simulations with the Lipid14 [25] and the ECC-lipid models compared with experiments [?].

14. Increase the height of the order parameter figure

15.  $sn-1$  and  $sn-2$  order parameters should be somehow labelled in the order parameter figure. Maybe empty and filled points?

16. Add size of the error bars in simulations to the caption.

17. Would it be possible to increase the size of points for acyl chain order parameters only in  $z$ -direction such that it would correspond the error bars?

18.  $x$ -axis in form factor plot from 0 to 0.6, where experimental data ends.  $y$ -axis from 0 to  $\sim 2.5$  to remove the empty space.

clusion, the ECC-lipid model reproduces the experimental dimensions of POPC lipid bilayer with the accuracy comparable to the other state of the art lipid models [36].

The acyl chain order parameters of the Lipid14 model [25] and the ECC-lipid model agree with the experimental values within the error bars in Fig. 1, although the ECC-lipid model gives slightly larger values for  $sn-1$  chain. Notably, the experimentally measured forking and small order parameter values of  $C_2$  segment in  $sn-2$  chain are relatively well reproduced by the both models. This has been suggested to indicate that the

carbonyl of  $sn-2$  chain is directed towards the water phase, in contrast to the carbonyl in  $sn-1$  chain, which would orient more along the bilayer plane [61–63]. While this may be an important feature for the ion binding details, it is not necessarily reproduced by the available lipid models [36].

The order parameters of  $\alpha$  and  $\beta$  carbons in the headgroup are slightly larger in the ECC-lipid model than in the Lipid14 model, which is apparently related to the P-N vector orienting  $7^\circ$  more toward the water phase in the ECC-lipid model, see Fig. 2. With the current data we cannot, however, conclude which one of the models give the more realistic headgroup conformations. The ECC-lipid model gives the  $\beta$  carbon order parameter value closer to experiments, while value for  $\alpha$  carbon is better in the Lipid14 model. Despite of some deviations from the experimental order parameter values in Fig. 1, the accuracy of the both models in the glycerol backbone region is comparable to the other state of art lipid models available in literature [35].

20. Dynamics check is missing: MSD (Hector/Joe)

## B. Calibration of lipid electrometer: Response of POPC head groups to bound charge

Before proceeding to the ion binding affinity, we quantify the response of the headgroup order parameters to the amount of bound charge by using mixtures of monovalent cationic surfactants (dihexadecyldimethylammonium) and POPC [34]. The amount of bound charge per PC in these systems is given by the molar fraction of cationic surfactants, because essentially all surfactants with two hydrophobic acyl chains can be assumed to locate in the lipid bilayers. The experimental data for these systems can be used to validate the sensitivity of lipid headgroup order parameters to the amount of bound charge in simulations.

The changes of the headgroup order parameters with an increasing amount of the cationic surfactant is compared between experiments [34] and simulations in Fig. 2. Approximately linear decrease of the order parameters, as expected from Eq. 3, is observed in simulations and experiments at least for the mole fractions below  $\sim 30\%$ . The slope is, however, too steep in the Lipid14 model indicating that the headgroup order parameters respond too sensitively to the bound positive charge. The slope in the ECC-lipid model is in very good agreement with experiments for the  $\alpha$  segment, while the slope is slightly underestimated for the  $\beta$  segment.

The headgroup P-N vector angle with respect to the membrane normal is also shown in Fig. 2 as a function of the mole fraction of the cationic surfactant. As suggested previously [20], the headgroup orients more towards the water phase with the increasing amount of positive charge in a PC lipid bilayer. The effect is more pronounced in the Lipid14 model, for which the addition of 50% mole fraction of the cationic surfactant leads to the decrease of  $20^\circ$  of the P-N vector angle, while the corresponding change in the ECC-lipid model is  $11^\circ$ . The difference is in line with the smaller order parameter changes and the reduced charge-dipole interactions in the latter model. The lesser sensitivity of the P-N vector an-

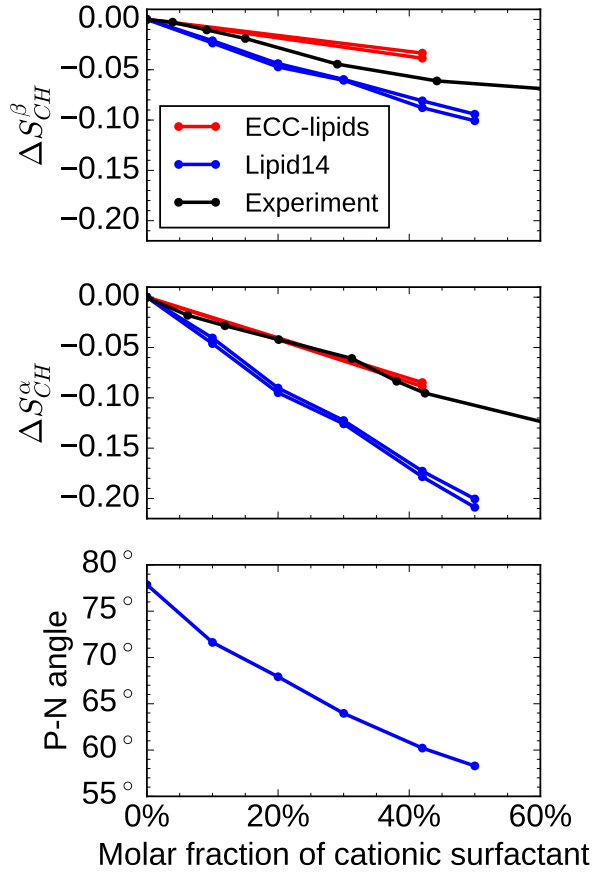


FIG. 2: The changes of headgroup order parameters and P-N vector orientation as a function of cationic surfactant (dihexadecyldimethylammonium) in POPC bilayer from simulations and experiments [34].

- 21. Labeling should be consistent with the previous figure, i.e. experimental data with diamonds.
- 22. x-axis scale from -1 to 51 to make the point in zero fully visible and to remove empty space.
- 23. Empty space between figures and from the right column could be reduced.

gle response in the ECC-lipid model can be considered to be more realistic, because the changes of the headgroup order parameters as a function of the bound positive charge are in better agreement with experiments in this model. The results also imply that the validation and improvements of MD simulation models are generally required for the reliable simulation studies of the lipid headgroup responses to ions or other biomolecules, as also concluded previously [35].

### C. Cation binding affinities to POPC membrane validated through lipid electrometer

The changes of the lipid bilayer headgroup order parameter from different simulations and experiments [4, 5] are shown in Figs. 3 and 4 as a function of NaCl and  $\text{CaCl}_2$  concentrations. These results can be used to compare the ion bind-

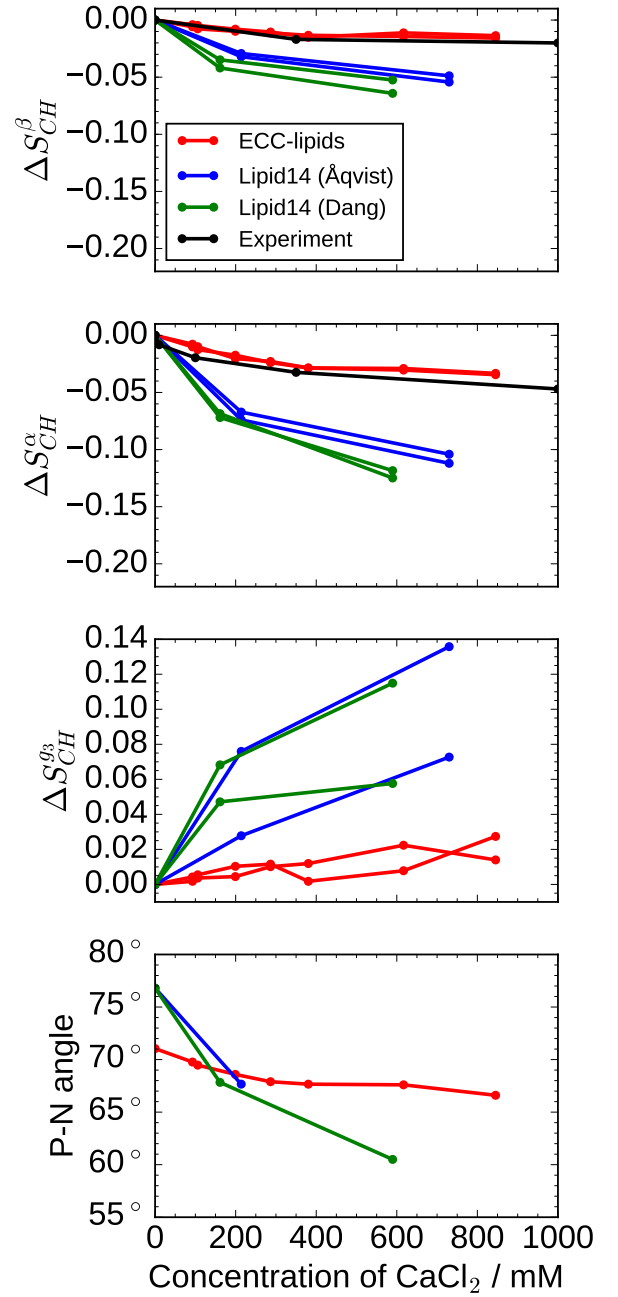


FIG. 3: Changes of head group order parameters of POPC bilayer as a function of  $\text{CaCl}_2$  concentrations are shown from simulations with different force fields together with experimental data (DPPC [4] and POPC [5]). Ion concentrations in bulk water are shown in x-axis. Values from simulations are calculated from the of cation number density  $C_{np}$  from the region at the simulation box edge with the constant ion concentration as  $[\text{ion}] = C_{np}/0.602$ . Simulation data with Lipid14 and Åqvist ion parameters is taken directly from Ref. [18].

- 24. I think that we must show the NaCl results in the main paper. I think that the best would be to use similar two column format, which we had before. This is used also in NMRlipids II and makes the comparison easier
- 25. The DPPC and POPC should be shown and properly labelled as we had previously.
- 26. The labeling should be consistent with previous figures, i.e., experiments with diamonds.
- 27. Start x-axis scale from -1 to make the point in zero fully visible.
- 28. Start y-axis scale of the two top figures from -0.13 to remove the empty space.
- 29. y-axis scale of the bottom figure from 59 to 78 to remove the empty space.
- 30. Empty space between figures and from the right column could be reduced.
- 31. Experimental values from [4] to be put in the  $g_3$  figure: the value of  $g_3$  order parameter of DPPC was -0.214 in the absence of ions [average of two closely spaced splittings] and -0.211 in the presence of 0.35 M  $\text{CaCl}_2$  (at 59 Celcius). No effect of ions could be detected on DPPC bilayers labeled at the C-2 segments of both fatty acyl chains.”

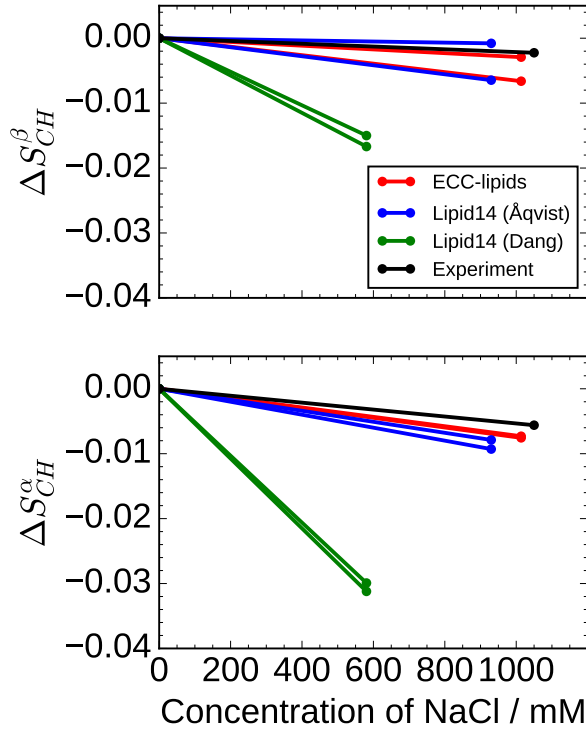


FIG. 4: Changes of head group order parameters  $\alpha$  and  $\beta$  of POPC bilayer as a function of NaCl concentrations are shown from simulations with different force fields together with experimental data [4]. Ion concentrations in bulk water are shown in x-axis. Values from simulations are calculated from the of cation number density  $C_{np}$  from the region at the simulatin box edge with the constant ion concentration as  $[\text{ion}] = C_{np}/0.602$ . Simulation data with Lipid14 and Åqvist ion parameters is taken directly from Ref. [18].

ing affinities to lipid bilayers between simulations and experiments by using the electrometer concept, because the order parameters decrease proportionally to the amount of bound positive charge [18, 20]. The recent comparison of different simulation models to the experimental data revealed that most models significantly overestimate the  $\text{Na}^+$  ion binding to PC lipid bilayers and that none of the available models correctly reproduce the details of the binding of  $\text{Ca}^{2+}$  ions [18]. A positive exception was the Lipid14 model [25] simulated with Åqvist ions, as seen from the data replotted from Ref. 18 in Figs. 3 and 4. The model reproduced the experimentally measured small order parameter changes with NaCl and imperceptible  $\text{Na}^+$  binding to PC bilayers [4, 5]. However, the changes of the headgroup order parameters as a function of  $\text{CaCl}_2$  concentration were overestimated by the same combination of force field parameters.

Since significant artefacts are reported in simulations with Åqvist ions is water [? ], we also simulated the Lipid14 model with the ion models by Dang et al. [50–52] and ECC-ions [22, 24?] having more realistic bulk behaviour. Instead of the improvement in the binding behaviour, we observed overbinding also of  $\text{Na}^+$  with these ions models, while the results with  $\text{Ca}^{2+}$  were barely affected, as seen in Figs. 3 and

TABLE II: The relative surface excess and the probabilities of contacts between bound Calcium and different oxygen moieties in POPC from different simulation models. The  $\text{CaCl}_2$  concentration of the ions in water is 350mM in the analyzed systems

model	$\Gamma_{Ca}^w (\text{nm}^{-2})$	$P_{\text{PO}_4}^{\text{Ca}^{2+}}$	$P_{\text{O}_{carb.}}^{\text{Ca}^{2+}}$
ECC-lipids	$0.07 \pm 0.01$	99%	25%
Lipid14/Åqvist	$0.13 \pm 0.01$	-	-
Lipid14/Dang	$0.3 \pm 0.03$	-	-

S??**.32.Add OP-response of Lipid14+ECC-ions plot in SI.** The results are in line with the previous work [18], suggesting that the improvements in the lipid parameters are required to correctly describe the divalent cation binding to PC lipid bilayers.

The results from the simulations with the ECC-lipid and the ECC-ion models [22, 24?] exhibit an improved behaviour of cation binding to a POPC bilayer in Fig. 3, showing a good agreement with experiments in the changes of the lipid headgroup order parameters as a function of NaCl and  $\text{CaCl}_2$  concentrations. Since also the headgroup order parameter response the to the bound positive charge the ECC-lipid model was in good agreement with experiments in section III B, we conclude that the model correctly reproduces the binding affinity of  $\text{Na}^+$  and  $\text{Ca}^{2+}$  ions to POPC lipid bilayer. Furthermore, the overestimated lipid headgroup order parameter changes of POPC in the Lipid14 model as a function of  $\text{CaCl}_2$  concentration arise from both, the overestimated binding affinity and sensitivity of the headgroup tilt to the bound positive charge. This probably applies also to the other lipid models considered in the previous study [18], emphasizing the importance of the comparison of the lipid headgroup order parameter response to the bound charge between simulations and experiments as done in section III B.

**33.SAMULI: Maybe we should discuss the repeat distances and area per molecules measured at [8, 9, 64]**

#### D. Cation binding to POPC membrane in atomistic detail

The binding affinities of  $\text{Ca}^{2+}$  ions to POPC bilayer in different simulation models were quantified by calculating the relative surface excess using Eq. 4 and the bulk concentrations determined from the density profiles in Fig. 5. All these simulation have the same, 350 mM, concentration of  $\text{CaCl}_2$  with respect to water (concentration before solvating the lipids in experiments). As expected from the changes of the lipid headgroup order parameters in Fig. 3, the relative surface excess for the ECC-lipid model,  $\Gamma_{Ca}^w = 0.07 \pm 0.01 \text{nm}^{-2}$ , is significantly smaller than for the Lipid14 model with Åqvist ions,  $\Gamma_{Ca}^w = 0.13 \pm 0.01 \text{nm}^{-2}$ , or with Dang ions,  $\Gamma_{Ca}^w = 0.3 \pm 0.03 \text{nm}^{-2}$ . **34.JOE: I'd put the  $\Gamma$  values into a table SAMULI: They are now in the table together with probabilities of the calcium binding probabilities to different POPC oxygens. However, I am not sure if there the table is useful in the end.** Interestingly, the relative surface excess of NaCl at 1 M concentration (ECC-ions [22]) calculated using density profiles in Fig. ?? is qualitatively different from  $\text{CaCl}_2$  having a negative value  $\Gamma_i^w = -0.1 \pm 0.01 \text{nm}^{-2}$ , meaning that wa-

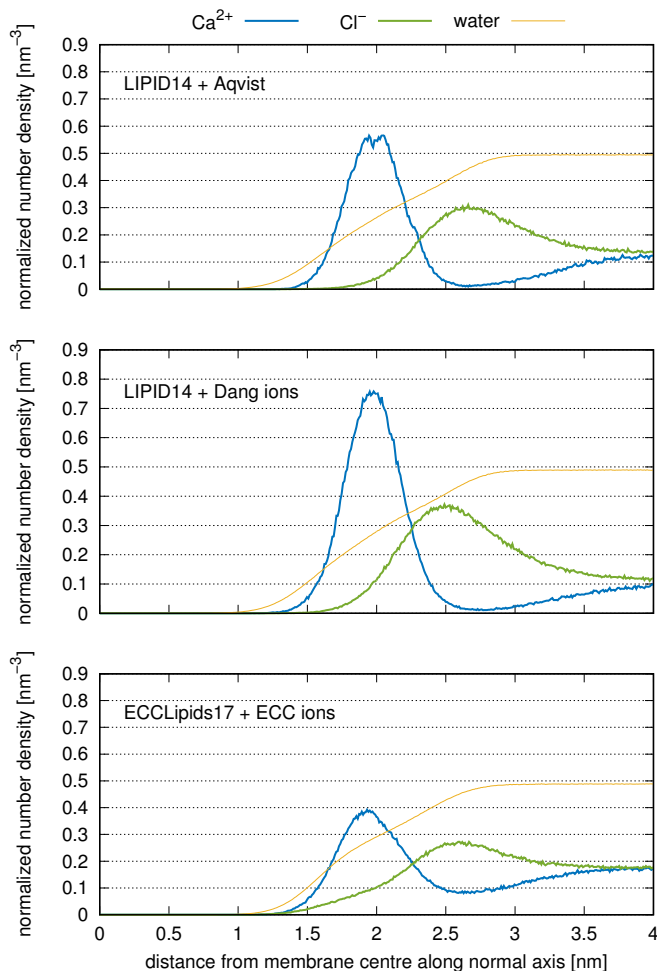


FIG. 5: Number density of  $\text{Ca}^{2+}$  and  $\text{Cl}^-$  as a function of membrane normal axis for different force fields. Data for Lipid14 with Åqvist ions are taken directly from Ref. 18. Densities of  $\text{Cl}^-$  and water are divided with 2 and 200, respectively, to visualize them with the same scale as  $\text{Ca}^{2+}$ . The molar concentration of the ions in water is 350 mM in all systems presented here.

36.PAVEL: draw phosphate position with its variance, add water density (scaled) and include the number of  $\Gamma$ -surface access.

37.JOE: Change the figure so that it contains a membrane background

ter molecules are preferred to sodium and chloride ions at the membrane-water interface. This is in contrast to the most of the available lipid force fields, which predict a specific binding of sodium on PC lipid bilayers [18]. 35.Densities and relative surface excess from NaCl systems to be added. The discussion above to be finished after this.

The interactions between ions and different oxygen moieties of POPC, were analyzed by calculating the probability of the contacts with the smaller or equal distance than 0.3 nm, as done previously in Ref. 14. The results are shown in Table 35. The probability for the bound  $\text{Ca}^{2+}$  ions to be in contact with the phosphate oxygens is 99%, indicating the interactions of Calcium ions purely with carbonyl oxygens has the probability of less than 1%. However, the probability for the bound  $\text{Ca}^{2+}$  ion to be in contact with carbonyl oxygen is 25%, in-

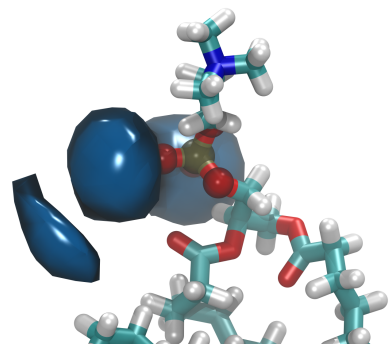


FIG. 6: Contours of probability isodensities of  $\text{Ca}^{2+}$  with respect to the phosphate oxygens of POPC from ECC-lipid simulation.

38.JOE: I'll update this figure with some ensemble of configuration to support binding preference of  $\text{Ca}^{2+}$  SAMULI: I am not sure if this would be needed anymore.

dicating that roughly quarter of the bound Calcium ions are in close contact with both, phosphate and carbonyl oxygens. It should be noted that in this analysis carbonyl and phosphate may or may not belong to the same lipid, and the carbonyl chain locate in either of the acyl chains. While the higher concentrations of  $\text{CaCl}_2$  naturally increased the amount of contacts per lipid, the distribution of contacts between phosphate and carbonyl oxygens was not affected. The most likely contacts between  $\text{Ca}^{2+}$  ions and phosphate oxygens is visualized with the probability isodensity contours in Fig. 6.

Even though the  $\text{Na}^+$  ions bind to POPC bilayer with the very low probability, it is possible to analyze the distribution of contacts from simulations with a large sodium concentration of 1000 mM. The results show that the sodium ions bind purely to the phosphate oxygens of POPC with the probability of 55% and purely to the carbonyl oxygens with the probability of 20%, leaving the probability of 25% for the simultaneous binding to both, phosphate and carbonyl oxygens.

In conclusion, the results suggest that the Calcium ions specifically bind to phosphate oxygens, while occasionally interacting also with carbonyls. This is in good agreement with the previous conclusions based in large amount of experimental and theoretical studies [3, 7, 15–17], but slightly updates the picture given by the previous MD simulation, where the binding to carbonyls was found to be more pronounced [10, 11, 13, 14]. Also the Sodium ions bind most likely to the phosphate oxygens, while the probability of binding purely to carbonyls is also significant. The physiological relevance of the details of sodium binding is, however, uncertain due to the very weak binding.

#### E. Stoichiometry of binding of $\text{Na}^+$ and $\text{Ca}^{2+}$ cations to POPC membrane

The previous interpretation of the experimental data for the changes of lipid headgroup order parameters, shown in Fig. 3, concluded that the experimental data was best explained by the ternary complex binding model, where  $\text{Ca}^{2+}$  ion bind to



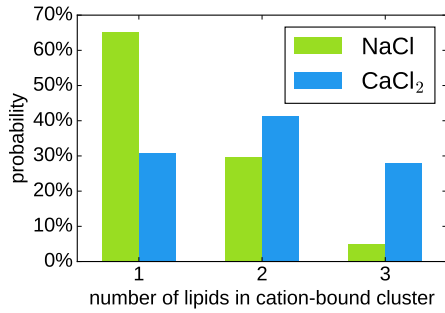


FIG. 7: Relative probabilities of existence of  $\text{Na}^+$  or  $\text{Ca}^{2+}$  complexes with a certain number of POPC lipids.  $\text{Na}^+$  complexes were evaluated from the simulation with 1 M concentration; and  $\text{Ca}^{2+}$  complexes were evaluated from the simulation with 287 mM concentration.

a POPC membrane with a stoichiometry 2 POPC:1  $\text{Ca}^{2+}$  [5]. However, also a Langmuir adsorption model (i.e. stoichiometry 1 POPC:1  $\text{Ca}^{2+}$ ) was successfully fit to the experimental data when only low concentrations of  $\text{CaCl}_2$  were considered [66]. These binding models and the measured headgroup order parameter changes are also included in the tabulated experimental binding constants [67].

Since the experimentally measured changes of the POPC lipid headgroup order parameters as a function of  $\text{CaCl}_2$  concentration are reproduced by the ECC-lipid model, it can be used to give more versatile interpretation of binding stoichiometry than the simple binding models. The stoichiometry was directly evaluated from simulations by calculating the relative propensities of various  $\text{Ca}^{2+}:n \times \text{POPC}$  complexes, which were defined to occur when cations and lipids were found within a cut off distance of 0.3 nm. The observed propensities of 42% for two lipids, 30% for one lipid, and 28% for three lipids are shown in Figure 7 for  $\text{Ca}^{2+}:n \times \text{POPC}$  complexes at 285 mM concentration. **39. Also the larger complexes were analysed, right? So we can write "Larger complexes were not existent in simulation.", or something like that?** While the ternary complex had the largest propensity, the complexes with 1 and 3 lipids occur with only a slightly lower probability, suggesting more complex binding stoichiometry than the simple ternary complex model. It should be, however, noted that on average one Calcium binds roughly to two lipids, because the probabilities of forming the complexes with 1 or 3 lipids are almost equal. This probably explains the successful fit of the ternary complex model to the experimental data. **40. I think that we either have to do the analysis in SI properly, i.e., using the real  $C_I$  from simulations or remove the sentence below and the related content from SI.** Ternary complex model also provides a good fit to our simulations with ECC-lipids (see Fig. 8 in SI and its caption for details).

Also the probabilities of different complexes formed by  $\text{Na}^+$  ions and POPC analyzed from the ECC-lipid model simulation with 1 M concentration of NaCl are shown in Fig. 7. In contrast to Calcium, the Sodium ions most likely binds to one POPC, while the probability to bind two lipids is less likely and very small for more than two.

## F. Residence times of $\text{Na}^+$ and $\text{Ca}^{2+}$ cations in POPC membrane

The residence time of  $\text{Ca}^{2+}$  in a POPC membrane is experimentally estimated to be lower than  $10 \mu\text{s}$  [5]. The recent MD simulations indicate that the equilibration of  $\text{Ca}^{2+}$  binding to POPC bilayer may take hundreds of nanoseconds [14], which could become an issue for the detailed binding studies with MD simulation trajectories with the having length less than several microseconds [18].

To analyze the residence time in the ECC-lipid model we **41. describe how the residence time analysis was done.** Histograms of the residence times analyzed from the ECC-lipid simulation and from the CHARMM36 simulation data **42. specify the system, POPC?** taken from the previous study [14] (the simulation data was downloaded from Ref. 65) are shown in Fig. S?? in SI. **43. JOE: Plot a histogram of residence times based on our simulations and simulation from 14 and put it into SI.**

**44. This paragraph should be clarified, but I cannot do it, because the residence time figure is not there yet.** In the CHARMM36 simulation approximately 20% of bound residence times of  $\text{Ca}^{2+}$  are limited by the length of the simulation, 800 ns, and only less than 60% of bound residence time is smaller than half of the simulation length, 400 ns. Other simulations with CHARMM36 and Slipids models reported in the previous work show even longer residence times. The ECC-lipids model estimates 90% of the residence times of calcium bound to a POPC membrane to be smaller than 60 ns, which is at least two orders of magnitude lower than for the CHARMM36. In addition, the longest observed residence time in the ECC-lipid simulation is 120 ns, which is well below the length of our simulations.

Interestingly,  $\text{Na}^+$  cations exhibit much more rapid exchange between membrane and solvent than calcium. The residence time of sodium bound to a POPC membrane is smaller than 2 ns for 90% of the time it is bound to the membrane with the longest measured bound time being 13 ns. Such an exchange between membrane and solvent is an order of magnitude faster than for calcium cations.

Such a finding changes the point of view on binding of calcium to PC membranes from a very strong long-term stable binding with rare exchanges to a relatively frequent exchange of calcium cations in equilibrium between membrane and solvent. The reduced barrier for the Calcium binding is also visible in the density distributions in Fig. 5, where the more shallow minimum for the Calcium density is observed at the interface.

### 1. Internal side-note:

However,  $\Sigma_{\text{O}_{\text{carb}}}^{\text{Ca}^{2+}}$  is increased in simulation with the highest  $\text{CaCl}_2$  concentration when carbonyl dipoles are scaled only with 0.945 (roughly done through charge redistribution) to :  $\Sigma_{\text{O}_{\text{carb}}}^{\text{Ca}^{2+}} \approx 0.08$ .

The average number of contacts per lipid between  $\text{Ca}^{2+}$  and any oxygen atom in POPC is  $\Sigma_{\text{O}}^{\text{Ca}^{2+}} = 0.264 \rightarrow 0.309$ , whereas if only phosphate oxygen atoms are considered the

average number of contacts decreases only by a tiny amount to  $\Sigma_{\text{PO}_4}^{\text{Ca}^{2+}} = 0.262 \rightarrow 0.303$ , and if only carbonyl oxygen atoms are considered (phosphate oxygens contribute, but are not counted as contacts), this value is merely  $\Sigma_{\text{carb.}}^{\text{Ca}^{2+}} = 0.066 \rightarrow 0.139$ .

This means that calcium is in contact with a phosphate oxygen for 98% of the time it is bound to the membrane, whereas 46% of the time accounts for contact with a carbonyl oxygen, and purely carbonyl bound states account for less than 2% of configurations. The states that have a contribution from carbonyl oxygens also contain a bound phosphate, so it can be thought of rather as a stabilizing moiety.

The residence times change to 75ns (90% of bound time) and max is 185ns. That's not much, too. It certainly is not a game changer, I'd even call it to be within accuracy. The slight problem may be that with this tweak, there's approx. 17% more cations bound to the membrane, which means, I'd need to tune the sigma parameter a bit (increase the scaling factor  $f_\sigma$ ). That could detune the membrane structure... Not  $f_q$  – that's set by the simulations with the surfactant. Good. I think that such a binding detail is within the accuracy of the proposed simple correction. It would be worth noting that the model may underestimate slightly the contribution from carbonyls due to this. But we can't say to what extent...

#### IV. CONCLUSIONS

By using the electrometer concept we show that the binding of  $\text{Na}^+$  and  $\text{Ca}^{2+}$  ions to a POPC lipid bilayer can be accurately described with the classical MD simulation force field, where the electronic polarization is implicitly included using the electronic continuum correction (ECC) [21]. The proposed ECC-lipids model is a significant improvement over other available lipid models, which all overestimate specific cation binding affinities [18]. While the structural details of a POPC lipid bilayer simulated with the ECC-lipids model agree with experiments with the comparable accuracy to the other state of the art lipid models, it also reproduces the experimental lipid head group order parameter responses to the cationic surfactant, NaCl and  $\text{CaCl}_2$  concentrations.

The good agreement with experiments enables the atomic resolution interpretation of NMR experiments by using MD simulations. In agreement with previous interpretations of experimental data [7, 15–17], the  $\text{Ca}^{2+}$  ions mainly interact with phosphate oxygens. However, the stoichiometry of the binding is significantly more complicated than in the previous interpretation of the NMR data based on the ternary complex model, where one calcium binds to two POPC molecules [5]. The complexes of one calcium bound to two lipids are the most probable also in the ECC-lipids model, but the complexes of one or three lipids per one calcium were observed to be almost equally likely. While the success of the ternary complex model is understandable based on the simulation results, a simple binding model cannot detect the complex binding observed in the simulation.

The improved cation binding behaviour to POPC bilayer pave the way for simulations of complex biochemical systems

with correctly described electrostatic interactions in the vicinity of cellular membranes. The ECC-lipids model is build by scaling the partial charges and the LJ-radius of the head-group, glycerol backbone and carbonyl atoms of the Lipid14 POPC model [25]. While the Lipid14 model is compatible with the AMBER force field family, the compatibility of the ECC-lipids model may be compromised due to the changes in intermolecular interactions of the scaled atoms. On the other hand, a fully consistent ECC-force field should include the correction also in other than lipid molecules, including water. The work toward this direction and the extension to other lipid molecules and force fields is left for the future studies.

This work can be reached as a repository containing all data at `zenodo.org:\dots\dots\dots`.

#### Acknowledgments

P.J. acknowledges support from the Czech Science Foundation (grant no. 16-01074S) and 600 from the Academy of Finland via the FiDiPro award.

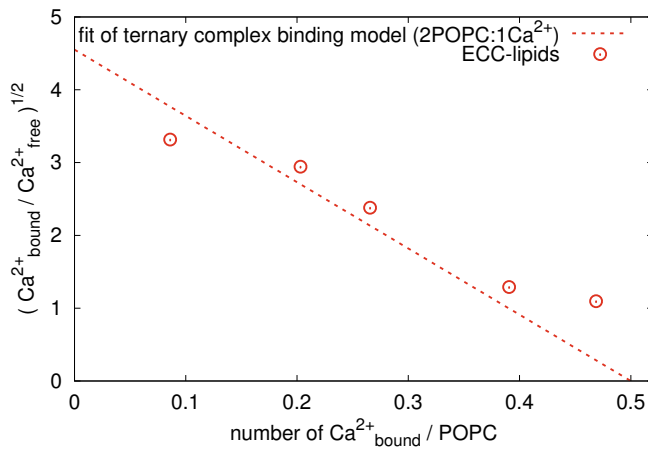


FIG. 8: Ternary complex binding model of  $\text{Ca}^{2+}$  to a POPC membrane that assumes the stoichiometry of 2 POPC:1  $\text{Ca}^{2+}$  (details in reference 5) provides a good fit to experimental measurements [5] and it also provides a good fit to our simulation data. Note that the units in the reference 5 are different from the units presented here, and, hence, the observed slope of the linear relationship is different.

## SUPPLEMENTARY INFORMATION

It was found in the original work [5] that a ternary complex binding model (i.e. 2 POPC:1  $\text{Ca}^{2+}$ ) provides the best fit to experimental measurements of all considered models in that study. In such a model, there is a linear relationship between quantities  $C_b$ , mole fraction of bound  $\text{Ca}^{2+}$  per POPC, and  $\sqrt{C_b/C_I}$ , where  $C_I$  is the concentration of free cations at the plane of ion binding [5]. The concentration  $C_b$  was obtained from an extrapolation of linear relation between deuterium NMR measurements and atomic absorption spectroscopy for low concentrations of  $\text{CaCl}_2$ . Such an extrapolation is valid as long as the mode of  $\text{Ca}^{2+}$  binding remains constant throughout the extrapolation range. The concentration  $C_I$  is determined by using the surface potential by using the Boltzmann equation. However, Boltzmann theory yields inaccurate results for divalent cations like  $\text{Ca}^{2+}$  [68]. An atomistic simulation, on the other hand, provides these quantities directly without severe assumptions. **45. Did you really calculate the  $C_I$  from simulations without severe assumptions? Note that this concentration at the plane of binding, which do not equal the concentration of free cations.** Hence we hypothesise that the discrepancy between the results in the experiment [5] and our simulations likely lays in the fact that the assumptions and relations used for determining concentrations  $C_b$  and  $C_I$  in the experiment [5] gradually do not hold for higher concentrations of  $\text{Ca}^{2+}$ .

- [1] P. Scherer and J. Seelig, The EMBO journal **6** (1987).
- [2] J. Seelig, Cell Biol. Int. Rep. **14**, 353 (1990), URL [http://dx.doi.org/10.1016/0309-1651\(90\)91204-H](http://dx.doi.org/10.1016/0309-1651(90)91204-H).
- [3] G. Cevc, Biochim. Biophys. Acta - Rev. Biomemb. **1031**, 311 (1990).
- [4] H. Akutsu and J. Seelig, Biochemistry **20**, 7366 (1981).
- [5] C. Altenbach and J. Seelig, Biochemistry **23**, 3913 (1984).
- [6] J.-F. Tocanne and J. Teissie, Biochim. Biophys. Acta - Reviews on Biomembranes **1031**, 111 (1990).
- [7] H. Binder and O. Zschörnig, Chem. Phys. Lipids **115**, 39 (2002).
- [8] G. Pabst, A. Hodzic, J. Strancar, S. Danner, M. Rappolt, and P. Laggner, Biophys. J. **93**, 2688 (2007).
- [9] D. Uhrkov, N. Kuerka, J. Teixeira, V. Gordeliy, and P. Balgav, Chemistry and Physics of Lipids **155**, 80 (2008).
- [10] R. A. Böckmann, A. Hac, T. Heimburg, and H. Grubmüller, Biophys. J. **85**, 1647 (2003).
- [11] R. A. Böckmann and H. Grubmüller, Ang. Chem. Int. Ed. **43**, 1021 (2004).
- [12] M. L. Berkowitz and R. Vacha, Acc. Chem. Res. **45**, 74 (2012).
- [13] A. Melcrov, S. Pokorna, S. Pullanchery, M. Kohagen, P. Jurkiewicz, M. Hof, P. Jungwirth, P. S. Cremer, and L. Cwiklik, Sci. Reports **6**, 38035 (2016).
- [14] M. Javanainen, A. Melcova, A. Magarkar, P. Jurkiewicz, M. Hof, P. Jungwirth, and H. Martinez-Seara, Chem. Commun. **53**, 5380 (2017), URL <http://dx.doi.org/10.1039/C7CC02208E>.
- [15] H. Hauser, M. C. Phillips, B. Levine, and R. Williams, Nature **261**, 390 (1976).
- [16] H. Hauser, W. Guyer, B. Levine, P. Skrabal, and R. Williams, Biochim. Biophys. Acta - Biomembranes **508**, 450 (1978), ISSN 0005-2736, URL <http://www.sciencedirect>.

TABLE III: Area per lipid (APL) from different models of POPC with no ions

model	APL ( $\text{\AA}^2$ )	Temperature [K]
Lipid14	$65.1 \pm 0.6$	300
Lipid14 [25]	$65.6 \pm 0.5$	303
ECC-lipids		
OPC3	$62.2 \pm 0.6$	300
OPC3	$64.2 \pm 0.6$	313
SPC/E	$65.1 \pm 0.6$	313
OPC	$64.4 \pm 0.6$	313
TIP4p/2005	$66.8 \pm 0.6$	313
experiment	62.7	293
experiment [60] <b>46.REF</b>	64.3	303
experiment	67.3	323
experiment	68.1	333

**47. Result with normal TIP3P missing?**

- com/science/article/pii/0005273678900913.
- [17] L. Herbert, C. Napolitano, and R. McDaniel, Biophys. J. **46**, 677 (1984).
- [18] A. Catte, M. Giryach, M. Javanainen, C. Loison, J. Melcr, M. S. Miettinen, L. Monticelli, J. Maatta, V. S. Oganessian, O. H. S. Ollila, et al., Phys. Chem. Chem. Phys. **18** (2016).
- [19] R. Vacha, S. W. I. Siu, M. Petrov, R. A. Böckmann, J. Barucha-Kraszewska, P. Jurkiewicz, M. Hof, M. L. Berkowitz, and P. Jungwirth, J. Phys. Chem. A **113**, 7235 (2009).
- [20] J. Seelig, P. M. MacDonald, and P. G. Scherer, Biochemistry

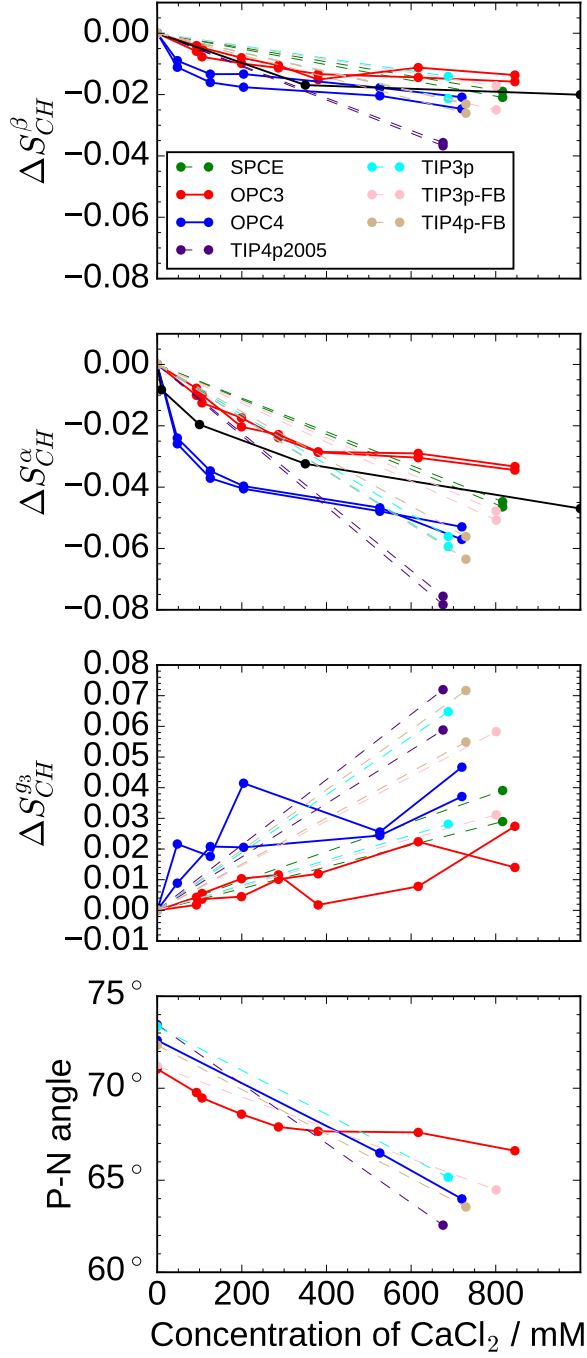


FIG. 9: Changes of head group order parameters of POPC bilayer as a function of  $\text{CaCl}_2$  concentrations are shown from simulations with different force fields and water models together with experimental data (DPPC [4] and POPC [5]). Ion concentrations in bulk water are shown in x-axis. Values from simulations are calculated from the of cation number density  $C_{np}$  from the region at the simulation box edge with the constant ion concentration as  $[\text{ion}] = C_{np}/0.602$ .

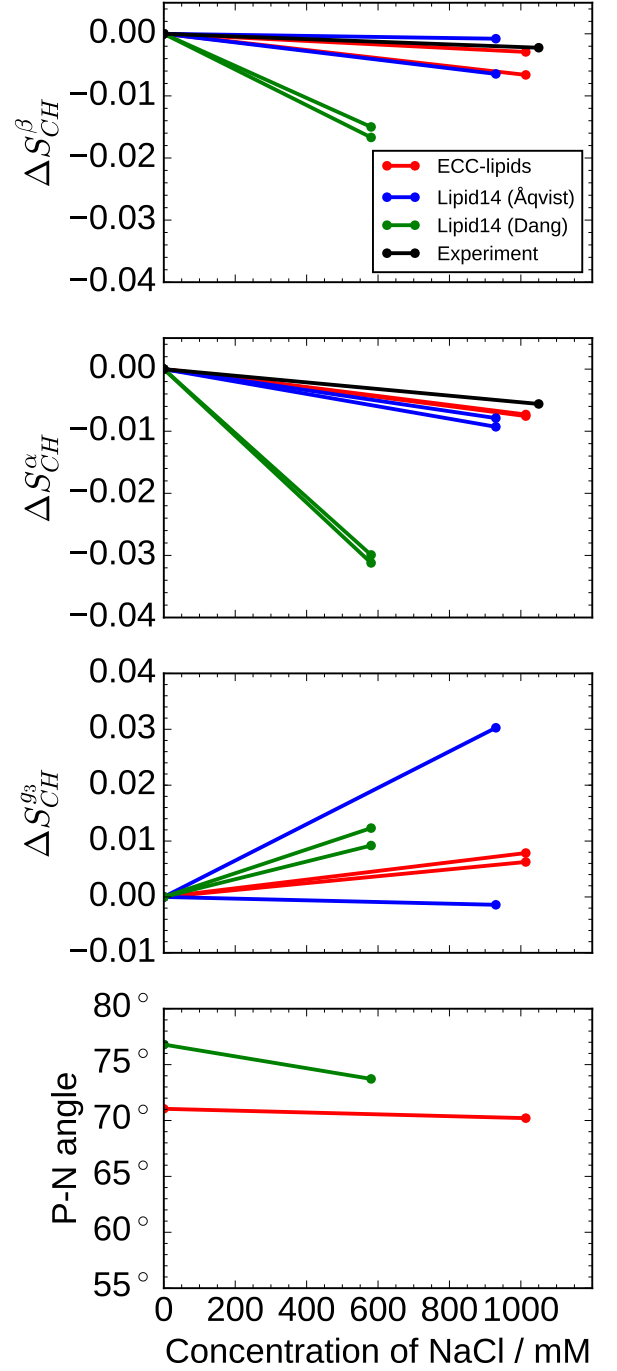


FIG. 10: Changes of head group order parameters of POPC bilayer as a function of  $\text{NaCl}$  concentrations are shown from simulations with different force fields together with experimental data [4]. Ion concentrations in bulk water are shown in x-axis. Values from simulations are calculated from the of cation number density  $C_{np}$  from the region at the simulation box edge with the constant ion concentration as  $[\text{ion}] = C_{np}/0.602$ . Simulation data with Lipid14 and Åqvist ion parameters is taken directly from Ref. [18].



TABLE IV: Simulation parameters

simulation property	parameter
time-step	2 fs
equilibration time	100 ns
simulation time	200 ns
temperature	313 K
thermostat	v-rescale [69]
barostat	Parrinello-Rahman, semi-isotropic [70]
long-range electrostatics	PME [71]
cut-off scheme	Verlet [72]
Coulomb and VdW cut-off	1.0 nm
constraints	LINCS, only hydrogen atoms [73]
constraints for water	SETTLE [74]

- 26, 7535 (1987).
- [21] I. Leontyev and A. Stuchebrukhov, Phys. Chem. Chem. Phys. **13**, 2613 (2011).
- [22] E. Pluhaová, H. E. Fischer, P. E. Mason, and P. Jungwirth, Molecular Physics **112**, 1230 (2014), ISSN 0026-8976, URL <http://www.tandfonline.com/doi/abs/10.1080/00268976.2013.875231>.
- [23] M. Kohagen, P. E. Mason, and P. Jungwirth, J. Phys. Chem. B **118**, 7902 (2014).
- [24] M. Kohagen, P. E. Mason, and P. Jungwirth, J. Phys. Chem. B **120**, 1454 (2016).
- [25] C. J. Dickson, B. D. Madej, A. Skjervik, R. M. Betz, K. Teigen, I. R. Gould, and R. C. Walker, J. Chem. Theory Comput. **10**, 865 (2014).
- [26] J. Chowdhary, E. Harder, P. E. M. Lopes, L. Huang, A. D. MacKerell, and B. Roux, J. Phys. Chem. B **117**, 9142 (2013).
- [27] B. Jonsson, O. Edholm, and O. Teleman, J. Chem. Phys. **85**, 2259 (1986).
- [28] E. Egberts, S.-J. Marrink, and H. J. C. Berendsen, European Biophysics Journal **22**, 423 (1994).
- [29] I. V. Leontyev and A. A. Stuchebrukhov, The Journal of chemical physics **130**, 085102 (2009), ISSN 1089-7690, URL <http://scitation.aip.org/content/aip/journal/jcp/130/8/10.1063/1.3060164>.
- [30] I. V. Leontyev and A. A. Stuchebrukhov, Journal of Chemical Theory and Computation **6**, 1498 (2010), ISSN 1549-9618, URL <http://dx.doi.org/10.1021/ct9005807>.
- [31] H. Hu, Z. Lu, and and Weitao Yang\*, Journal of Chemical Theory and Computation **3**, 1004 (2007), ISSN 1549-9618, URL <http://dx.doi.org/10.1021/ct600295n>.
- [32] C. C. I. Bayly, P. Cieplak, W. D. Cornell, and P. a. Kollman, The Journal of Physical ... **97**, 10269 (1993), ISSN 0022-3654, 93/2091- 10269\$04.00/0, URL <http://pubs.acs.org/doi/abs/10.1021/j100142a004>.
- [33] U. C. Singh and P. A. Kollman, Journal of Computational Chemistry **5**, 129 (1984), ISSN 1096987X.
- [34] P. G. Scherer and J. Seelig, Biochemistry **28**, 7720 (1989).
- [35] A. Botan, F. Favela-Rosales, P. F. J. Fuchs, M. Javanainen, M. Kanduč, W. Kulig, A. Lamberg, C. Loison, A. Lyubartsev, M. S. Miettinen, et al., J. Phys. Chem. B **119**, 15075 (2015).
- [36] O. S. Ollila and G. Pabst, *Atomistic resolution structure and dynamics of lipid bilayers in simulations and experiments* (2016), in Press, URL <http://dx.doi.org/10.1016/j.bbamem.2016.01.019>.
- [37] D. S. Cerutti, J. E. Rice, W. C. Swope, and D. A. Case, The Journal of Physical Chemistry B **117**, 2328 (2013), pMID: 23379664, <http://dx.doi.org/10.1021/jp311851r>, URL <http://dx.doi.org/10.1021/jp311851r>.
- [38] A. Maciejewski, M. Pasenkiewicz-Gierula, O. Cramariuc, I. Vattulainen, and T. Rog, J. Phys. Chem. B **118**, 4571 (2014).
- [39] (???)
- [40] T. M. Ferreira, R. Sood, R. Bärenwald, G. Carlström, D. Topgaard, K. Saalwächter, P. K. J. Kinnunen, and O. H. S. Ollila, Langmuir **32**, 6524 (2016).
- [41] A. Seelig and J. Seelig, Biochemistry **16**, 45 (1977).
- [42] J. H. Davis, Biochim. Biophys. Acta - Reviews on Biomembranes **737**, 117 (1983).
- [43] G. Beschiaschvili and J. Seelig, Biochim. Biophys. Acta - Biomembranes **1061**, 78 (1991).
- [44] D. K. Chattoraj and K. S. Birdi, *Adsorption at the Liquid Interface from the Multicomponent Solution* (Springer US, Boston, MA, 1984), pp. 83–131, ISBN 978-1-4615-8333-2, URL [https://doi.org/10.1007/978-1-4615-8333-2\\_4](https://doi.org/10.1007/978-1-4615-8333-2_4).
- [45] S. Izadi and A. V. Onufriev, Journal of Chemical Physics **145**, 074501 (2016), ISSN 00219606, URL <http://aip.scitation.org/doi/10.1063/1.4960175>.
- [46] S. Izadi, R. Anandakrishnan, and A. V. Onufriev, The Journal of Physical Chemistry Letters **5**, 3863 (2014), ISSN 1948-7185, 1408.1679, URL <http://pubs.acs.org/doi/10.1021/jz501780a>.
- [47] H. J. C. Berendsen, J. R. Grigera, and T. P. Straatsma, Journal of Physical Chemistry **91**, 6269 (1987), ISSN 0022-3654, URL <http://links.isiglobalnet2.com/gateway/Gateway.cgi?GWVersion=2\&\&SrcAuth=mekentosj\&\&SrcApp=Papers\&\&DestLinkType=FullRecord\&\&DestApp=WOS\&\&KeyUT=A1987K994100038\&\&5Cnpapers2://publication/uuid/17978EF7-93C9-4CB5-89B3-086E5D2B9169\&\&5Cnhttp://pubs.acs.org/doi/pdf/10.1021/>.
- [48] L. P. Wang, T. J. Martinez, and V. S. Pande, Journal of Physical Chemistry Letters **5**, 1885 (2014), ISSN 19487185, URL <http://pubs.acs.org/doi/abs/10.1021/jz500737m>.
- [49] J. L. Abascal and C. Vega, The Journal of chemical physics **123**, 234505 (2005), ISSN 00219606, URL <http://aip.scitation.org/doi/10.1063/1.2121687>.
- [50] D. E. Smith and L. X. Dang, J. Chem. Phys **100** (1994).
- [51] T.-M. Chang and L. X. Dang, J. Phys. Chem. B **103**, 4714 (1999), ISSN 1520-6106, URL <http://dx.doi.org/10.1021/jp982079o>.
- [52] L. X. Dang, G. K. Schenter, V.-A. Glezakou, and J. L. Fulton, J. Phys. Chem. B **110**, 23644 (2006), ISSN 1520-6106, URL <http://dx.doi.org/10.1021/jp064661f>.
- [53] J. Aqvist, The Journal of Physical Chemistry **94**, 8021 (1990), URL <http://dx.doi.org/10.1021/j100384a009>.
- [54] M. Gyrch and O. H. S. Ollila, *Popc-amber.lipid14-verlet* (2015), URL <http://dx.doi.org/10.5281/zenodo.30898>.
- [55] M. J. Abraham, T. Murtola, R. Schulz, S. Páll, J. C. Smith, B. Hess, and E. Lindah, SoftwareX **1-2**, 19 (2015), ISSN 23527110, URL <http://www.sciencedirect.com/science/article/pii/S2352711015000059>.
- [56] A. K. Malde, L. Zuo, M. Breeze, M. Stroet, D. Poger, P. C. Nair, C. Oostenbrink, and A. E. Mark, Journal of Chemical Theory and Computation **7**, 4026 (2011).
- [57] D. Case, D. Cerutti, T. Cheatham, III, T. Darden, R. Duke,

- T. Giese, H. Gohlke, A. Goetz, D. Greene, et al., *AMBER 2017* (2017), university of California, San Francisco.
- [58] A. W. SOUSA DA SILVA and W. F. VRANKEN, *ACPYPE - AnteChamber PYthon Parser interfAcE*. (2017), manuscript submitted.
- [59] T. M. Ferreira, F. Coreta-Gomes, O. H. S. Ollila, M. J. Moreno, W. L. C. Vaz, and D. Topgaard, *Phys. Chem. Chem. Phys.* **15**, 1976 (2013).
- [60] J. P. M. Jämbbeck and A. P. Lyubartsev, *J. Phys. Chem. B* **116**, 3164 (2012).
- [61] A. Seelig and J. Seelig, *Biochim. Biophys. Acta* **406**, 1 (1975).
- [62] H. Schindler and J. Seelig, *Biochemistry* **14**, 2283 (1975).
- [63] K. Gawrisch, D. Ruston, J. Zimmerberg, V. Parsegian, R. Rand, and N. Fuller, *Biophys. J.* **61**, 1213 (1992).
- [64] H. I. Petrache, S. Tristram-Nagle, D. Harries, N. Kucerka, J. F. Nagle, and V. A. Parsegian, *J. Lipid Res.* **47**, 302 (2006).
- [65] M. Javanainen, *POPC with varying amounts of cholesterol, 450 mM of CaCl<sub>2</sub>. Charmm36 with ECC-scaled ions* (2017), URL <https://doi.org/10.5281/zenodo.259376>.
- [66] P. M. Macdonald and J. Seelig, *Biochemistry* **26**, 1231 (1987).
- [67] D. Marsh, *Handbook of Lipid Bilayers, Second Edition* (RSC press, 2013).
- [68] D. Andelman, in *Handbook of biological physics* (Elsevier Science, 1995), vol. 1, chap. 12, pp. 603–642, URL <http://hwiki.liebel-lab.org/wiki/images/9/90/AndelmannReview.pdf>.
- [69] G. Bussi, D. Donadio, and M. Parrinello, *J. Chem. Phys.* **126** (2007).
- [70] M. Parrinello and A. Rahman, *J. Appl. Phys.* **52**, 7182 (1981).
- [71] T. Darden, D. York, and L. Pedersen, *J. Chem. Phys.* **98** (1993).
- [72] S. Páll and B. Hess, *Computer Physics Communications* **184**, 2641 (2013), ISSN 0010-4655, URL <http://www.sciencedirect.com/science/article/pii/S0010465513001975>.
- [73] B. Hess, H. Bekker, H. J. C. Berendsen, and J. G. E. M. Fraaije, *J. Comput. Chem.* **18**, 1463 (1997).
- [74] S. Miyamoto and P. A. Kollman, *J. Comput. Chem.* **13**, 952 (1992).

### ToDo

1. We should also cite papers where empirical scaling was used ionic liquids - but there the factor is not 0.5. . . . . 2
2. This needs a citation . . . . . 2
3. JOE: following discussion shall be modified in the enlightenment of our recent ECC-discussions. . . . . 2
4. missing REF for APL experiment . . . . . 2
5. We should discuss how this can potentially affect the intermolecular interaction when mixing scaled and non scaled molecules. JOE: I think that we rather increasingly see that there's nothing like "fully non-scaled" with the exception of ions with integer charges. So the discussion shall be rather more about the interaction of our "scaled" (I'd still rather call it ECC-corrected or whatever) and "semi-scaled" models. SAMULI: There is now a paragraph in the conclusions, which mentions this topic. . . . . 3

### P.

6. As Hector suggested, it might be better to write the simpler form for this equation. . . . . 4
7. More justification for the choosing the OPC3 water model are needed. It might be good to show the comparison with the scattering data in bulk water in SI. . . . . 4
8. The normal TIP3P was tested as well, right? . . . . . 4
9. Which water model was used in these simulations? . . . . . 4
10. To be uploaded to Zenodo . . . . . 4
11. To be added . . . . . 4
12. JOE: We cannot present an intricate cool new model for a lipid and claim at the same time that we can't simulate bromide. . . . . 4
13. Which water model was used in these simulations? . . . . . 4
14. Parameters are available at ?? . . . . . 4
15. Increase the height of the order parameter figure . . . . . 5
16. sn-1 and sn-2 order parameters should be somehow labelled in the order parameter figure. Maybe empty and filled points? . . . . . 5
17. Add size of the error bars in simulations to the caption. . . . . 5
18. Would it be possible to increase the size of points for acyl chain order parameters only in z-direction such that it would correspond the error bars? . . . . . 5
19. x-axis in form factor plot from 0 to 0.6, where experimental data ends. y-axis from 0 to ~2.5 to remove the empty space. . . . . 5
20. put original references, not Slipids param. paper. . . . . 5
21. Dynamics check is missing: MSD (Hector/Joe) . . . . . 5
22. Labeling should be consistent with the previous figure, i.e. experimental data with diamonds. . . . . 6
23. x-axis scale from -1 to 51 to make the point in zero fully visible and to remove empty space. . . . . 6
24. Empty space between figures and from the right column could be reduced. . . . . 6
33. Add OP-response of Lipid14+ECC-ions plot in SI . . . . . 6
34. SAMULI: Maybe we should discuss the repeat distances and area per molecules measured at [8, 9, 64] . . . . . 6
25. I think that we must show the NaCl results in the main paper. I think that the best would be to use similar two column format, which we had before. This is used also in NMRlipids II and makes the comparison easier . . . . . 7
26. The DPPC and POPC should be shown and properly labelled as we had previously. . . . . 7
27. The labeling should be consistent with previous figures, i.e., experiments with diamonds. . . . . 7
28. Start x-axis scale from -1 to make the point in zero fully visible. . . . . 7
29. Start y-axis scale of the two top figures from -0.13 to remove the empty space. . . . . 7
30. y-axis scale of the bottom figure from 59 to 78 to remove the empty space. . . . . 7
31. Empty space between figures and from the right column could be reduced. . . . . 7

32. Experimental values from [4] to be put in the $g_3$ figure: the value of $g_3$ order parameter of DPPC was -0.214 in the absence of ions [average of two closely spaced splittings] and -0.211 in the presence of 0.35 M $\text{CaCl}_2$ (at 59 Celcius). No effect of ions could be detected on DPPC bilayers labeled at the C-2 segments of both fatty acyl chains.” . . . . .	7	40. Also the larger complexes were analysed, right? So we can write “Larger complexes were not existent in simulation.”, or something like that? . . . . .	9
37. PAVEL: draw phosphate position with its variance, add water density (scaled) and include the number of $\Gamma$ -surface access. . . . .	8	41. I think that we either have to do the analysis in SI properly, i.e., using the real $C_I$ from simulations or remove the sentence below and the related concent from SI. . . . .	9
38. JOE: Change the figure so that it contains a membrane background . . . . .	8	42. describe how the residence time analysis was done	9
35. JOE: I’d put the $\Gamma$ values into a table SAMULI: They are now in the table together with probabilities of the calcium binding probabilities to different POPC oxygens. However, I am not sure if there the table is useful in the end. . . . .	8	43. specify the system, POPC? . . . . .	9
36. Densities and relative surface excess from NaCl systems to be added. The discussion above to be finished after this. . . . .	8	44. JOE: Plot a histogram of residence times based on our simulations and simulation from 14 and put it into SI. . . . .	9
39. JOE: I’ll update this figure with some ensemble of configuration to support binding preference of $\text{Ca}^{2+}$ SAMULI: I am not sure if this would be needed anymore. . . . .	8	45. This paragraph should be clarified, but I cannot do it, because the residence time figure is not there yet. . .	9
		46. Did you really calculate the $C_I$ from simulations without severe assumptions? Note that this concentration at the plane of binding, which do not equal the concentration of free cations. . . . .	11
		47. put original references, not Slipids param. paper. . .	11
		48. Result with normal TIP3P missing? . . . . .	11